University of Glasgow

Viavattene, G. and Ceriotti, M. (2022) Low-thrust, multiple NEA mission design with sample return to Earth using machine learning. *Journal of Spacecraft and Rockets*, 59(6), pp. 2148-2159.(doi: 10.2514/1.A34959)

The material cannot be used for any other purpose without further permission of the publisher and is for private use only.

There may be differences between this version and the published version. You are advised to consult the publisher's version if you wish to cite from it.

https://eprints.gla.ac.uk/277422/

Deposited on 07 October 2022

Enlighten – Research publications by members of the University of Glasgow
http://eprints.gla.ac.uk

Low-Thrust, Multiple NEA Mission Design with Sample Return to Earth using Machine Learning

Giulia Viavattene* and Matteo Ceriotti†
University of Glasgow, Glasgow G12 8QQ, United Kingdom

Sample return missions to near-Earth asteroids (NEAs) are invaluable for the scientific community to learn more about the initial stages of the solar system formation and life evolution. Low-thrust propulsion technology enables missions with multiple asteroid rendezvouses to collect samples and eventually return to Earth, thanks to its high specific impulse. To identify the best asteroid sequences with return to Earth, this work proposes to employ machine learning techniques and, specifically, artificial neural networks (ANNs), to quickly estimate the cost of each transfer between asteroids. The ANN is integrated within a sequence search algorithm based on a tree search, which identifies the asteroid sequences and selects the best ones in terms of propellant mass required and interest value. This algorithm can design NEA sequences so that specific asteroids of interest, for which a sample return would be more valuable, can be targeted. A pseudospectral optimal control solver is then used to find the optimal trajectory and control history. The performance of the proposed methodology is assessed by analyzing three distinctive NEA sequences ending with return to Earth and rendezvous. Near-term low-thrust propulsion enables to rendezvous five asteroids, and return samples to Earth in about ten years from launch. It is demonstrated that visiting more scientifically-interesting asteroids increases the appeal of the sequence at the cost of more propellant mass required.

Nomenclature

a = semi-major axis, m

a_d = albedo, -

A = appealing factor, -

$\mathbf{a_T}$ = acceleration, m/s^2

b = ANN biases

d = asteroid diameter, m

e = eccentricity

*Ph.D. Candidate, James Watt School of Engineering, James Watt (South) Building; g.viavattene.1@research.gla.ac.uk.
†Senior Lecturer, James Watt School of Engineering, James Watt (South) Building; Matteo.Ceriotti@glasgow.ac.uk.

f, g = in-plane modified equinoctial elements

$\mathcal{F}^l$ = ANN activation function

g_0 = standard gravitational acceleration, m/s^2

i = inclination, deg

I_{sp} = specific impulse, s

I_V = interest value, -

H = absolute magnitude, -

h, k = out-of-plane modified equinoctial elements

J = performance index

L = true longitude, deg

m = spacecraft mass, kg

M = mean anomaly, deg

$\mathbf{N}$ = thrust direction vector

n_{rev} = number of revolutions

p = semilatus rectum, m

R = correlation coefficient, -

$\mathbf{r}$ = Sun-spacecraft position vector, m

t = time, s

$t0, f$ = time of flight, s

T_{max} = maximum thrust, N

T_{train} = network training time, s

$\mathbf{u}$ = control vector

$\mathbf{x}$ = state vector

w = ANN weights

$\mathbf{y}$ = ANN output vector

$\mathbf{y}_t$ = ANN target output vector

α = interest weight coefficient, -

ΔV = velocity increment, km/s

$\mathcal{E}$ = error, -

μ = gravitational parameter, m^3/s^2

I. Introduction

The first successful sample return missions were the Apollo Moon missions and the Russian Luna 16, 20 and 24 missions, launched between 1968 and 1976, which returned samples of the lunar surface to Earth, contributing to the understanding of the Moon's geological history and composition [1]. Similarly to studying samples of the Moon, the scientific community is interested in collecting samples from the surface of asteroids. It is expected that this will allow us to learn more about the initial stages of the solar system formation and how life began [2, 3].

To date, two missions have returned asteroid samples and one is on its return journey. The JAXA Hayabusa probe rendezvoused with an *S*-type asteroid 25143 Itokawa and, in November 2010, it returned an asteroid sample to Earth [4]. In 2014 JAXA launched the improved Hayabusa2 probe to visit the near-Earth *C*-type asteroid 162173 Ryugu. It took samples of the asteroid surface and returned to Earth in December 2020 [5]. The OSIRIS-REx mission was launched by NASA in 2016 to return samples from near-Earth asteroid (NEA) 101955 Bennu, and it has recently started its return to Earth [2].

Sample return missions to planets and small bodies represent one of the biggest challenges for space engineering. The velocity change ΔV required to complete this kind of missions can greatly outrun that of one-way missions and, according to the rocket equation, with increasing ΔV the propellant mass to complete the mission increases exponentially. Also, for a given spacecraft launch mass, a higher ΔV requires the payload mass fraction to be inevitably smaller so that more propellant can be carried on board, which consequently limits the maximum mass of samples which can be returned to Earth [6].

Rendezvousing multiple NEAs with sample return to Earth can increase the scientific return of those missions [7, 8]. Multiple NEA rendezvous (MNR) missions give the possibility of visiting a larger number of asteroids, from which samples can be extracted and returned to Earth for further studies. This kind of missions can thus reduce the cost with respect to employing multiple spacecraft to individual asteroids and returning samples.

MNR are highly demanding in terms of ΔV, which translates into changes in orbital energy, and they are even more so when followed by a return to Earth. For this reason, an efficient propulsion system is required to significantly keep the propellant mass ratio low. Low-thrust technologies, such as solar electric propulsion (SEP), are good candidates because of their high specific impulse [9, 10].

To design MNR mission trajectories, a complex global optimization problem needs to be solved, consisting of two coupled sub-problems [11]. The first is a large combinatorial sub-problem, which encodes the selection of the sequences of target asteroids [12]. To this end, trillions of permutations should be analyzed, since more than 22,000 NEAs are known to date, according to NASA's database*. The second sub-problem is continuous, and consists in finding the solution to an optimal control problem (OCP) to obtain the optimal flight trajectory to visit the selected asteroids with minimum propellant expenditure and/or time of flight (TOF). It should be stressed that the two problems cannot be

*Data available through the link `https://cneos.jpl.nasa.gov/orbits/elements.html` (accessed on 2020-01-10)

solved independently from each other, as the combinatorial part requires various inputs, such as the duration and cost of each transfer, which are obtained by solving the continuous sub-problem, and vice-versa. This study proposes to use machine learning to solve the continuous problem through estimates and, at the same time, tackle the combinatorial problem.

Asteroid-related problems were proposed in six out of the eight Global Trajectory Optimization Competitions (GTOC)[†]. The majority of the proposed solutions suggests the use of a simplified trajectory model to compute the asteroid sequence, while employing more accurate and complex methods to convert the obtained sequence into a feasible low-thrust trajectory. For instance, Peloni et al. [13] approximated low-thrust trajectories using a shape-based method and used a search-and-prune algorithm to find the sequence. Differently, a homotopic approach is used by Tang et al. [14], to quickly approximate the low-thrust transfers. Di Carlo et al. [15] proposed to traverse the asteroid belt with a high elliptical orbit and visit as many asteroids, which are encountered along that orbit, as possible.

In the past, machine learning was applied successfully to solve complex problems in aerospace sciences. Izzo et al. [16] surveyed the use of machine learning and artificial intelligence in domains such as interplanetary trajectory optimization, spacecraft guidance, and orbital prediction, anticipating a widespread use of these techniques. Dachwald [17] used artificial neural networks (ANNs) and evolutionary algorithms to compute the solar-sail trajectories to a NEA, showing that this method can explore the trajectory space search more exhaustively than traditional optimal control methods. Similarly, Hennes et al. [18] used machine learning to compute low-thrust transfers with minimum fuel mass between main-belt asteroids. Mereta et al. [19] employed machine learning techniques to estimate the final mass of a spacecraft flying a low-thrust trajectory between two NEAs, instead of solving the full OCP. Other applications include the increase of accuracy of pinpoint landing [20] and orbit prediction [21], and the design of MNR using solar sailing [22] or solar electric propulsion [23][24].

The purpose of this work is to prove the use an ANN to identify the most effective sequences of asteroids to visit and then return to Earth. It will be shown that a trained ANN can *quickly* estimate, in a fraction of the time needed by optimal control solvers, the cost and TOF of transfers using a near-term low-thrust propulsion system. This approach allows us to vastly reduce the computational time, compared to traditional optimization techniques [25].

The ANN is integrated within a sequence search algorithm based on a tree search which allows us to find solutions with a return to Earth within the maximum duration of the mission. The tree search allows to store the data in a organized structure of nodes and can explain well the sequential relationship between objects. Given the fast data search properties, similar tree-search-based algorithms were also used in the winning solutions of GTOC4 [26], GTOC5 [27] and second ranked solution of GTOC7 [28]. The algorithm, based on Peloni et al. [13], is enhanced so that the sequences can be evaluated and selected in terms of both propellant mass and interest value. Additionally, this algorithm can prioritize sequences so that specific asteroids of interest (a sample return would be more valuable) can be targeted.

[†]Data available through the link `https://sophia.estec.esa.int/gtoc_portal/` (accessed on 2020-01-10)

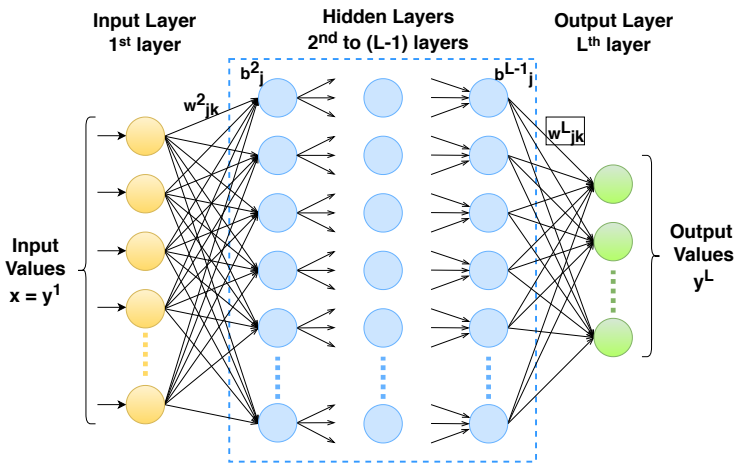

Fig. 1 Illustration of an ANN with L layers.

The paper is organized as follows. The ANN design is described in Sec. II, where the NEA database is generated and the architecture of the network is optimized for this application. In Sec. III, the sequence search algorithm is schematized and the logic is explained. The sequence search algorithm can be adjusted to target a specific asteroid within the sequence and to take into account the interest value of the asteroids visited. In Sec. IV NEA sequences with return to Earth are analyzed to assess the performance of the proposed methodology. Finally, Sec. V provides a summary of the methodology implemented and the results obtained.

II. Machine Learning for Low-thrust Transfers

Inspired by the biological cognitive systems of the animal brain, an ANN is a complex computing system that can model complex non-linear relationships to any degree of accuracy [29]. For function approximations, feedforward networks are preferred [30]. A neural network is organized in layers, where the information moves from the *input layer* to the *output layer* through a number of *hidden layers*. Each layer includes a defined amount of neurons and each neuron is connected directly to the neurons of the successive layer [31], as shown in Fig. 1.

The network is trained so that the mean squared error between the network outputs $\mathbf{y}$ and targets $\mathbf{y}_t$ is minimized:

$$\mathcal{E}_{MSE} = \frac{1}{N}\sum_{i=1}^{N} |\mathbf{y}_i - \mathbf{y}_{t,i}|^2 \tag{1}$$

with N being the number of outputs. Also, to ensure that the outputs fit well the targets, the correlation between the network outputs and targets is maximized, i.e., as close as possible to unity.

Designing a neural network for a particular application presents different challenges. Firstly, the identification of a method to generate the training database. Secondly, since the topology and hyper-parameters of the network influence the network accuracy, the values for each of these parameters, which offer the best network performance, need to be

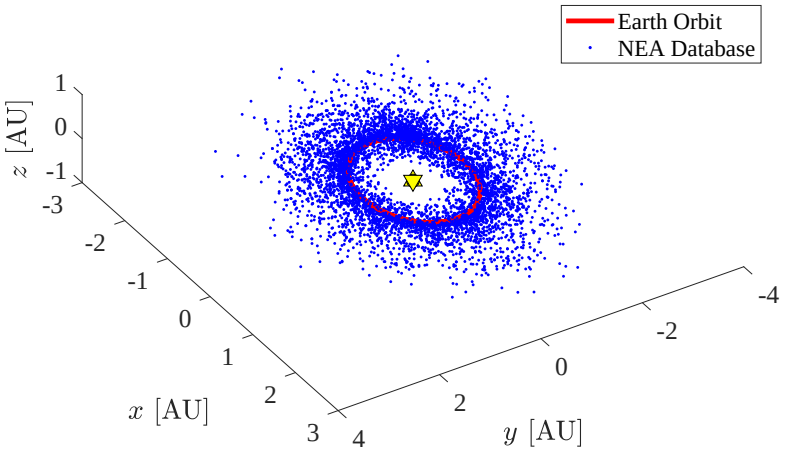

Fig. 2 NEAs selected for the generation of the training database.

identified. These points are addressed in the next two sections.

A. Training Database Generation

The training database contains the input vector and the target output vector. The input vector includes the orbital parametrization of the departure and arrival asteroids and the position along their orbits at a reference time. The target output vector includes the cost in terms of ΔV and TOF of the low-thrust, rendezvous transfers between the departure and arrival asteroids. It follows that the input vector $\mathbf{x}$ and output vector $\mathbf{y}$ can be defined as:

$$\mathbf{x} = [p_0, f_0, g_0, h_0, k_0, L_0, p_f, f_f, g_f, h_f, k_f, L_f] \tag{2}$$

$$\mathbf{y} = [\Delta V, t_{0,f}] \tag{3}$$

where $p_0, f_0, g_0, h_0, k_0, L_0$ and $p_f, f_f, g_f, h_f, k_f, L_f$ are the modified equinoctial elements (MEE) [32] describing the orbits of the departure and arrival NEAs, respectively, ΔV indicates the velocity increment and $t_{0,f}$ the time of flight. For the training of the network, the inputs and targets are normalized so that they have zero mean and unitary standard deviation.

For the generation of the database, NEAs which are of particular scientific interest for their composition and/or orbit are included, such as Potentially Hazardous Asteroids (PHA) and Near-Earth Object Human Space Flight Accessible Targets Study (NHATS). Figure 2 shows the 6,286 NEAs, which are used for the simulation, at their position (blue dots) with respect to the Earth's orbit (in red) on 27 April 2019. The orbital elements of these NEAs (*input*) are obtained from the NASA's Near-Earth Object Program.[‡]

To compute the ΔV and TOF of low-thrust transfers (*output*) between the couples of asteroids, an OCP needs to be

[‡]Data available through the link `https://cneos.jpl.nasa.gov/orbits/elements.html` (accessed on 2019-06-17)

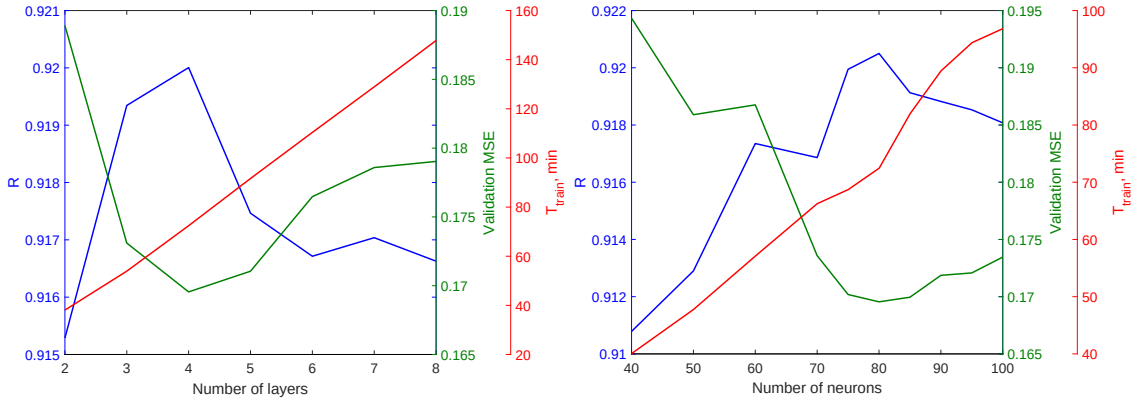

Fig. 3 Effect of varying the network parameters on the correlation coefficient R, validation-set MSE and training time.

solved. Considering that a sufficient number of samples is needed to accurately train the network, direct or indirect methods are excluded as they require a long computational time. Analytical methods can, instead, provide a quick and reliable, but approximated, trajectory description. For this work, the shape-based method [33] is chosen to approximate the shape of low-thrust transfers, for the given launch dates and propulsion system, and to estimate the ΔV and TOF. A genetic algorithm is used to compute the shaping parameters to obtain the rendezvous transfers with minimum cost. From the obtained acceleration profile, the control history can be retrieved.

The training database is built by permuting a subset of 100 NEAs and using the shape-based method to compute the cost and duration of the transfers between each couple of asteroids. All the departure dates are included in a launch window from January 2020 to December 2030. The training database comprises a total of 10,100 low-thrust transfers. The number of NEAs and the launch window are bounded for the generation of the training database. This is done to verify the *generalization* property of the neural network, for which a successfully trained ANN can generalize and estimate transfer costs between NEAs that are not included in the database and with different launch dates.

To verify the generalization property of the network, the database is divided into a training set, a validation set and a test set. The training set is used for the training, while the validation and test sets contain new samples that are not included in the training. The validation set is used to verify that the overfitting does not occur during the training, and the test set is used to test the performance of the network, after the training. To this end, the validation-set MSE is often considered when studying the network performance.

B. Network Architecture Design

The architecture of the network is defined by the number of hidden layers and the number of neurons. Other hyper-parameters of the network are the learning algorithm, activation function for each hidden layer, learning rate or gradient constant and its increase or decrease factor. Also, different orbit parametrizations can be used as inputs to the network, showing that different types of inputs can influence the performance of the network.

Table 1 Network architecture and hyper-parameters for the highest network performance.

ANN Parameter	Best value
Number of hidden layers	4
Number of neurons of each hidden layers	80
Learning algorithm	Levemberg-Marquardt
Activation function of each hidden layers	sigmoid
Gradient Constant μ	0.001
Decrease Factor μ_{dec}	0.1
Database division rates (training:validation:test)	70:15:15
Orbit parametrization for the network inputs	MEE

The effect of varying the hyper-parameters and the input of the network on its performance is studied with the purpose of identifying the combinations of parameter values that offer the highest network performance. Figure 3 shows the response of the network to varying the number of layers and neurons on the correlation coefficient R, MSE of the validation set and training time T_{train}. While the training time increases significantly as the number of layers and/or neurons increases, the performance of the network reaches a peak for a specific number of hidden layers and neurons.

A similar analysis is performed for each of the other network hyper-parameters and different orbit parametrizations used as input to the network. The interested reader can find a detailed description of these analyses in other publications [23, 24]. Table 1 presents the parameters of the network which led to the highest performance for this application, with a final correlation coefficient of 0.9732 and validation-set MSE of 0.1211.

III. Sequence Search Algorithm

The following sequence search algorithm is implemented to identify the most promising sequences of asteroids to visit and return to Earth. The logic of the algorithm is based on a *tree-search* method and breadth-first criterion so that all the possible NEA combinations for one leg are analyzed before exploring the successive leg, and so on. The algorithm is illustrated in Fig. 4. The search starts from Earth at a fixed launch date. The NEA database of N = 6,286 asteroids is loaded and their ephemerides are updated at the departure date $t_{0,i}$, where i indicates the i-th leg. The ANN is embedded within this algorithm to compute the cost and duration of low-thrust, rendezvous transfers from Earth to all the NEAs in the database. The N_S = 200 trajectories requiring the least propellant mass are stored. The maximum number of trajectories stored at each iteration is fixed to bound the complexity and required memory of the tree search, which grow exponentially as the number of sequences and/or objects increases. This allows for non-promising partial solutions to be discarded. I A stay time t_{stay} = 100 days is added at each object to allow enough time for rendezvous, close-up observation and/or sample collection. At this point, the arrival body becomes the departure body of the following leg and the same procedure is iterated for each trajectory.

A 10-year mission is divided into three phases and the selection of the next body to visit depends on each phase.

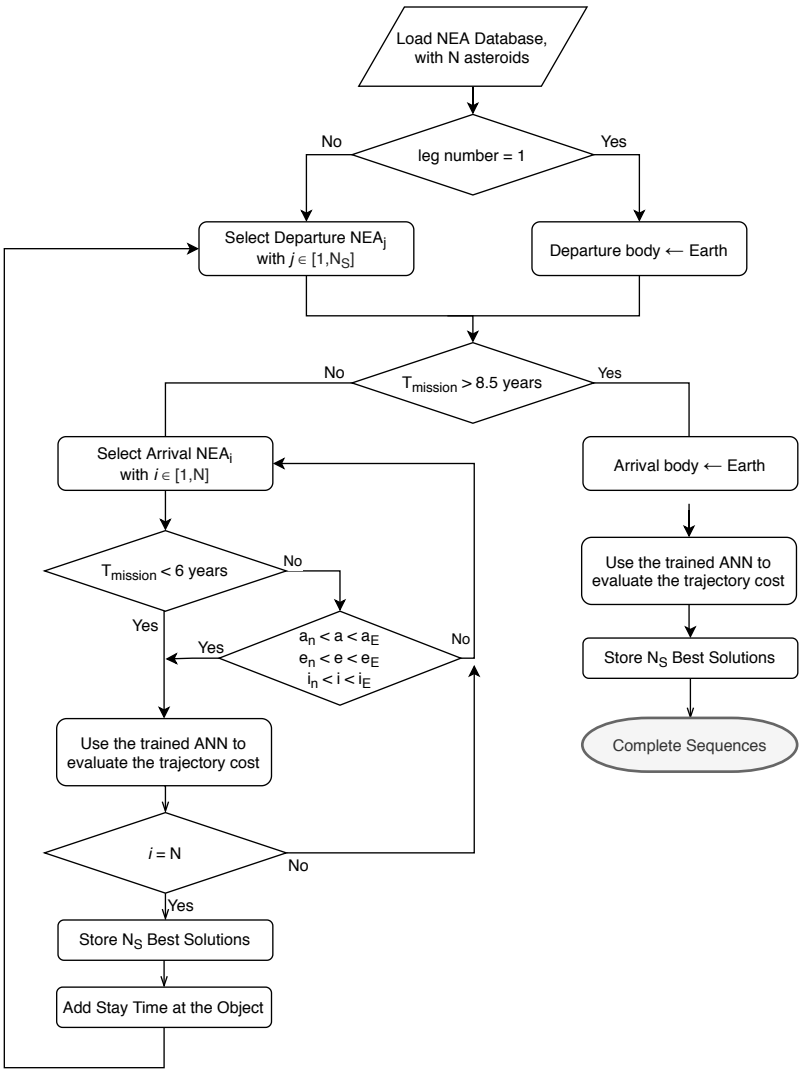

Fig. 4 Sequence search algorithm with return to Earth.

During the first phase, NEAs are selected based on the propellant mass consumption only. During the second phase, the NEAs are pruned so that the semi-major axis a, eccentricity e, and inclination i of the next visited NEA are included between those of the last-visited NEA and the Earth, i.e.:

$$a_n \leq a \leq a_E \tag{4}$$

$$e_n \leq e \leq e_E \tag{5}$$

$$i_n \leq i \leq i_E \tag{6}$$

where the subscript n indicates the n-th asteroid visited and E the Earth. In essence, this constrains the search to target

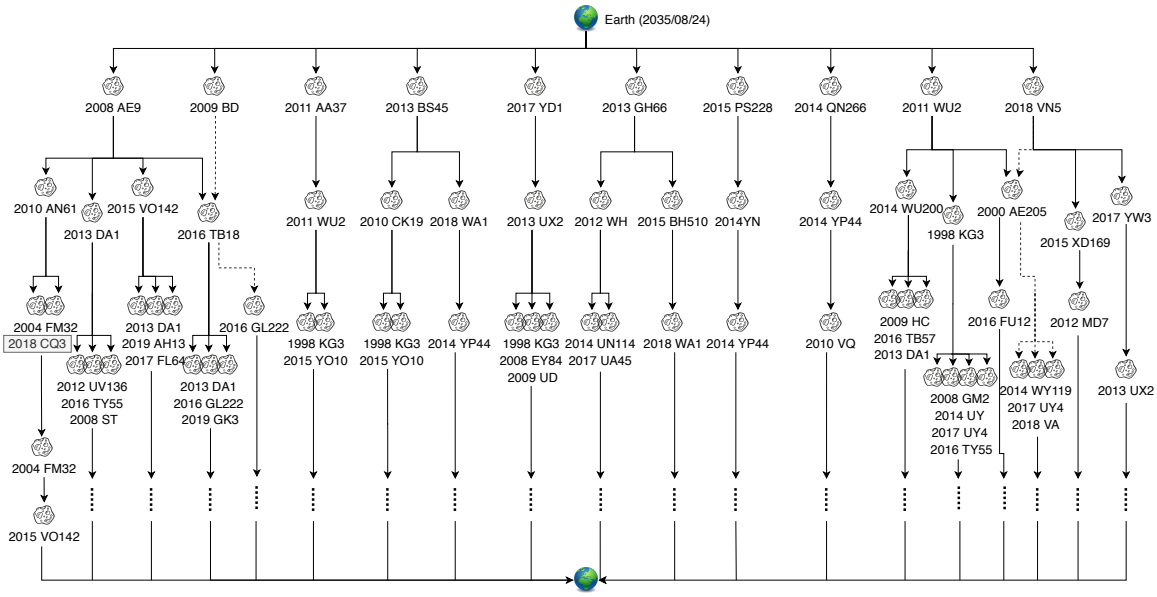

Fig. 5 Tree graph of the first three legs of sequences of five asteroids and with return to Earth (launch date: 24 August 2035). One complete sequence is shown.

asteroids which are incrementally more similar to Earth in terms of orbital elements. The expressions are defined for the case with $a_E \geq a_n$, $e_E \geq e_n$, and $i_E \geq i_n$, but they are inverted when the opposite case occurs. The pruning of the NEAs is performed after the mission duration of a partial sequence reaches 6 years (i.e., in the second half of the mission). At this point, NEAs are selected from the pruned dataset based on the ΔV required.

After the mission duration of a partial sequence reaches 8.5 years (value chosen to allow enough time for a feasible return leg for the 10-year mission), the third phase starts. It consists in the return to Earth (final leg), where Earth is targeted as the arrival body. Finally, the best solutions in terms of propellant mass expenditure are stored and considered as complete sequences.

Figure 5 shows sequences of five asteroids with return to Earth which were found by the sequence search algorithm for the departure date 24 August 2035. Since the number of permutations between asteroids grows rapidly with the number of legs, only the first three legs are plotted in full and, for illustration purposes, one complete sequence is fully shown.

A. Asteroid Targeting

The previous missions, which performed a sample return to Earth, were designed to target one asteroid which is reachable with the given propulsion system and particularly interesting from the scientific point of view. For instance, 25143 Itokawa and 162173 Ryugu were selected as the target asteroids for the missions Hayabusa and Hayabusa 2, respectively, because of their sizes and because they are reachable using an ion engine with a feasible ΔV [4, 5]. Similarly, NASA selected the asteroid 101955 Bennu for the mission OSIRIS-REx as it is rich in pristine carbonaceous

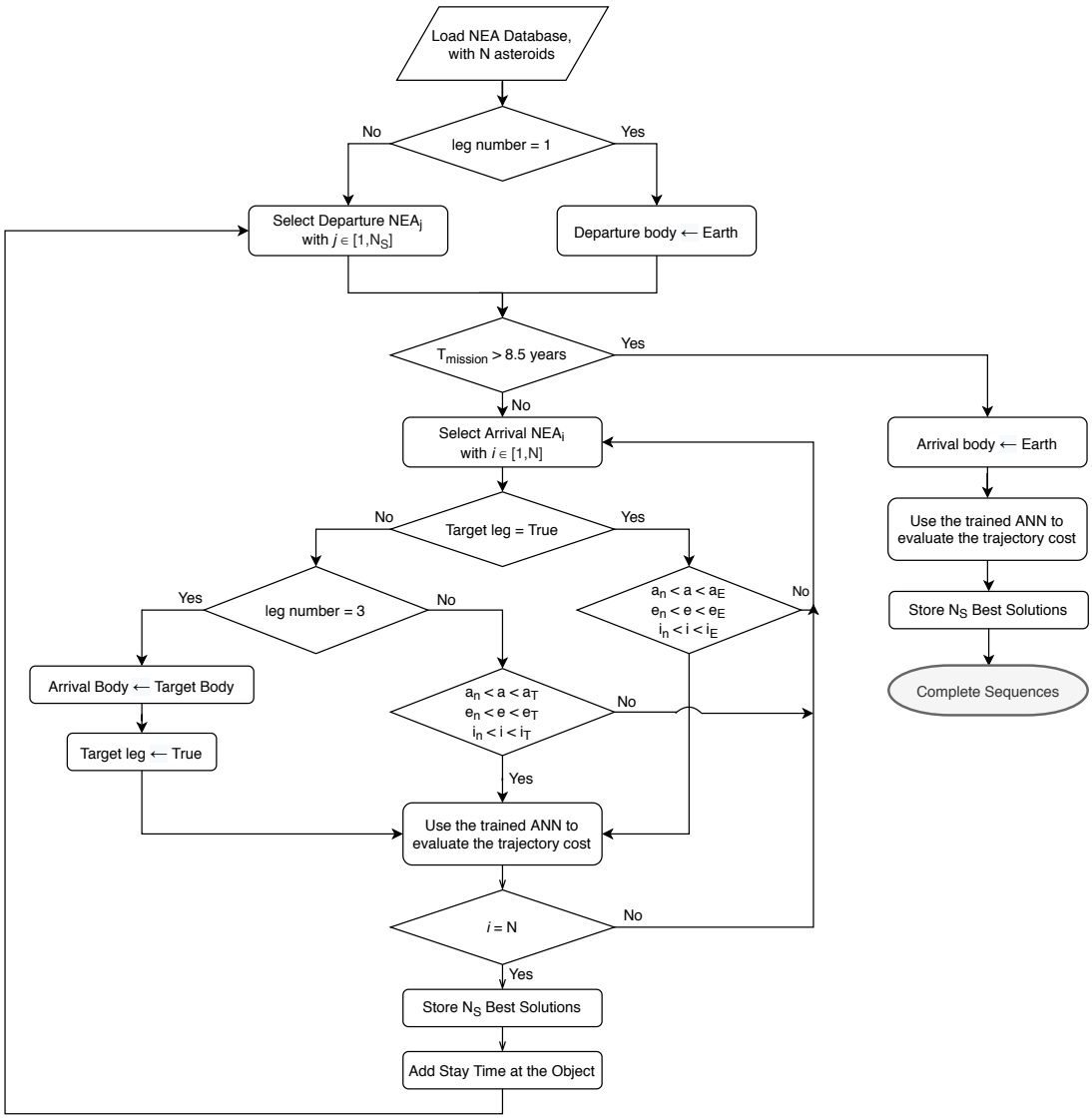

Fig. 6 Sequence search algorithm to target one NEA of interest and return to Earth.

material, which is a key element in organic molecules necessary for life [2]. In all the three missions, the asteroids were chosen primarily because the sample collections and analyses are expected to improve the knowledge on the formation and evolution of the planets and, in particular, of Earth, as well as the origin of water and organic matter.

The sequence search algorithm is enhanced in a way that enables to target a specific asteroid which is particularly interesting for the scientific community and for which a sample return would be more valuable. Figure 6 schematizes the algorithm which is implemented. Compared to the previous algorithm with no NEA targeting, this algorithm searches sequences so that the first half is focused on targeting the chosen asteroid of interest, while the second half is focused on targeting the Earth for a safe reentry. The purpose is to ensure that the spacecraft can reach the target asteroid and, simultaneously, visit as many asteroids as possible for observations and/or sample collections, while the spacecraft flies

from Earth to the target body and back to Earth. To this end, a pruning of the asteroids, which are visited between the departure from Earth and the arrival at the target body, is also performed. Only the NEAs with semimajor axis, eccentricity and inclination included between those of Earth and the target asteroid are considered, i.e.:

$$a_n \leq a \leq a_T \tag{7}$$

$$e_n \leq e \leq e_T \tag{8}$$

$$i_n \leq i \leq i_T \tag{9}$$

where n indicates the n-th asteroid visited (or Earth for the first leg) and T the targeted asteroid. After two legs have been identified, it is assumed that the spacecraft has reached an orbit from which it is possible to conveniently, in terms of cost and duration, transfer to the target body. Thus, the arrival body of the third leg is the target asteroid.

Once the target body is visited and the sample is collected, a second pruning of the asteroids, which are visited between the departure from the target body and the return to Earth, is performed. This is done, similarly to the previous algorithm represented in Fig. 4, to guarantee that the spacecraft can successfully return to Earth and visit as many asteroids as possible along its way back to Earth.

For the scenario presented in this work, asteroid 162173 Ryugu is targeted, which is a PHA and NHATS of the Apollo group with a diameter of approximately 1 km. This asteroid was previously chosen by JAXA for the Hayabusa2 mission as it has an unaltered or barely altered composition (C-type) and it is easily accessible from Earth [34]. Figure 7 shows the tree graph of the sequences of five asteroids, which target 162173 Ryugu in the third leg and, finally, return to Earth. These sequences are calculated by the sequence search algorithm for the departure date 24 August 2035.

B. Interest Value of NEA Sequences

As many asteroids remain *unclassified* due to the lack of quality data or limited opportunities for ground observation [35], we decided that NEAs, which are bigger in size, are more valuable to observe and return samples of. Larger asteroids are generally rarer and more suitable for landing and for the sample collection.

Apart from the asteroids which have been visited by a spacecraft in the past, the size and shape of most asteroids is yet unknown. Although most asteroids have irregular shape and only few of them are close to being spherical, the size of an asteroid can be estimated as the diameter of an equivalent sphere with a uniform surface, given its *absolute magnitude*, H, and assumed geometric albedo, a_d. The diameter (in km) of an asteroid can be estimated as follows [36]:

$$d = 10^{\left(3.1236 - 0.5 \log_{10}(a_d) - 0.2H\right)} \quad \text{[km]} \tag{10}$$

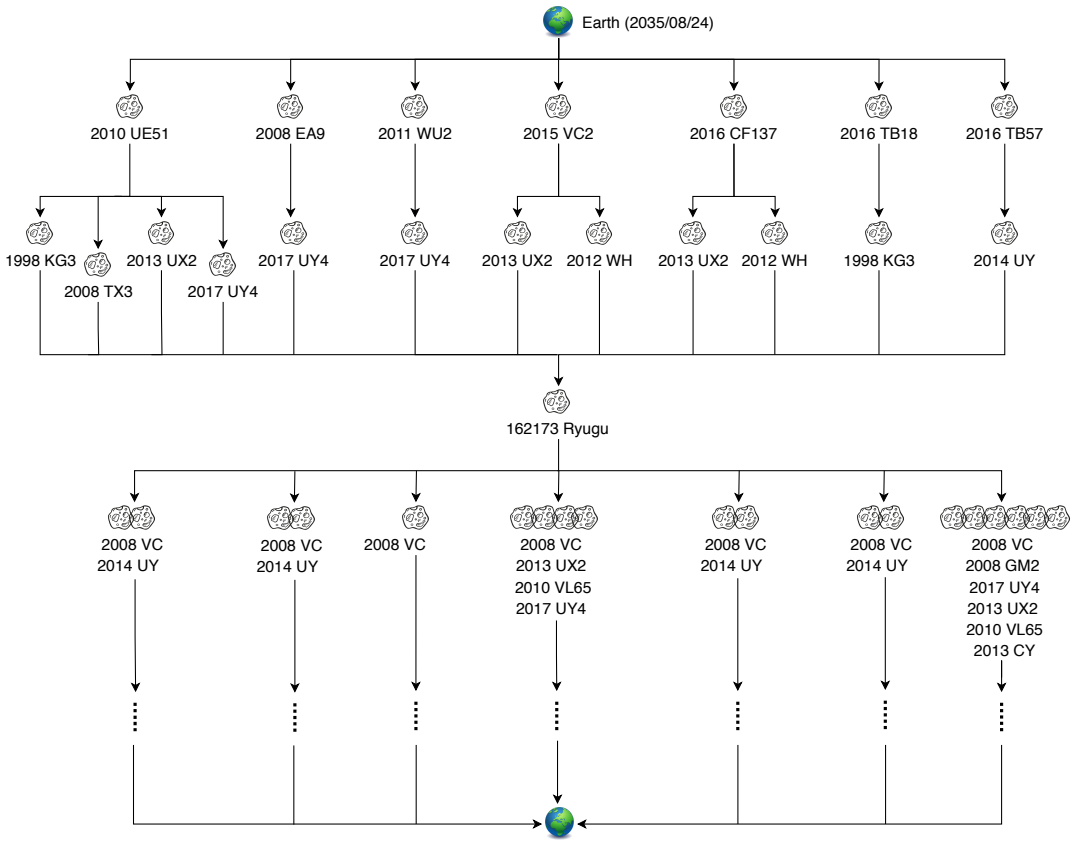

Fig. 7 Tree graph of the sequences targeting 162173 Ryugu in the third leg and visiting five asteroids before returning to Earth (launch date: 24 August 2035).

where the albedo, a_d, is generally assumed based on the spectral class corresponding to the assumed composition of the asteroid and an average value is typically used [37]. Due to the conceivable uncertainty in both H and a_d, Eq. (10) provides an approximate estimation of the size of an asteroid. For example, for the same absolute magnitude H, a deviation in albedo of 0.1 leads to an error in diameter by a factor of two.[§] However, considering that in Eq. (10) H has a larger impact than a_d in determining the asteroid's size, we will assume in the following that an asteroid with a smaller H is characterized by a larger size and represents a more interesting candidate to visit in a sequence.

To classify the obtained sequences on the basis of their scientific interest, the *interest value*, I_V, of each sequence is introduced and defined as the negative sum of the absolute magnitudes of all the visited asteroids, i.e.:

$$I_V = -\sum_{i=1}^{N_A} H_i \tag{11}$$

where H_i is the absolute magnitude of the i-th asteroid visited and $i \in [1, N_A]$, with N_A being the number of asteroids visited during the relative sequence. The greater the interest value, the larger the asteroids visited and the more interesting

[§]Data available through the NASA JPL Asteroid Size Estimator `https://cneos.jpl.nasa.gov/tools/ast_size_est.html` (accessed on 2020-07-14)

the sequence. It is important to underline that this choice is for the purpose of showing the validity of the method; the mission designer can select how to define the interest value of each sequence based on the mission objectives.

To take into account the interest value for the selection of the most convenient sequences to fly, during the sequence search, an *appealing factor A* is associated with each sequence as the weighted sum of its total ΔV and total I_V of the mission, which can be expressed as follows:

$$A = \alpha \Delta V_{n,tot} - (1 - \alpha) I_{V_n,tot} \tag{12}$$

where $\alpha \in [0, 1]$ is a weight coefficient representing the relative importance given to ΔV and I_V when selecting the sequences. Note that $\Delta V_{n,tot}$ and $I_{V_n,tot}$ refer to the normalized values of the total ΔV and I_V of the sequence. The sequence search algorithms are modified so that the $N_S = 200$ best trajectories characterized by the lowest A are selected, i.e., a compromise between minimum ΔV and maximum interest value.

Varying the value of the weight α and/or targeting one asteroid of interest within a sequence have an impact on the final mass expenditure and interest value of the sequence. Figures 8(a) and 8(b) show the distribution of the ΔV for all the transfers and ΔV_{tot} for all the sequences. Similarly, Figures 8(c) and 8(d) describe the distribution of the absolute magnitude, H, for all encountered NEAs and interest value, I_V, for all the sequences. These distributions are obtained when the sequence search algorithm is run for the following cases:

1) no target asteroid and $\alpha = 1$
2) 162173 Ryugu as the target asteroid and $\alpha = 1$
3) no target asteroids and $\alpha = 0.5$
4) 162173 Ryugu as the target asteroid and $\alpha = 0.5$

The figures indicate that when α is lower than one, i.e., the selection of the sequences is made on the basis of their I_V and ΔV, the selected sequences are characterized by a greater I_V and generally higher ΔV with respect to the case when only the ΔV is considered for the selection (i.e., $\alpha = 1$). For $\alpha = 1$ (cases (1) and (2)), it is possible to achieve a larger number of sequences with a greater I_V when an interesting asteroid is targeted within the sequences (case (2)). However, it should be noted that, when $\alpha < 1$ (cases (3) and (4)), the pruning of the asteroids, which is performed to ensure that the target asteroid can be conveniently reached, appears to reduce the likelihood to encounter asteroids with a larger size, compared to the case when no objects are targeted (case (3)). In summary, more interesting objects can be favored during the sequence selection process, increasing the overall appeal of the sequences generated by the search algorithm at the cost of a larger ΔV.

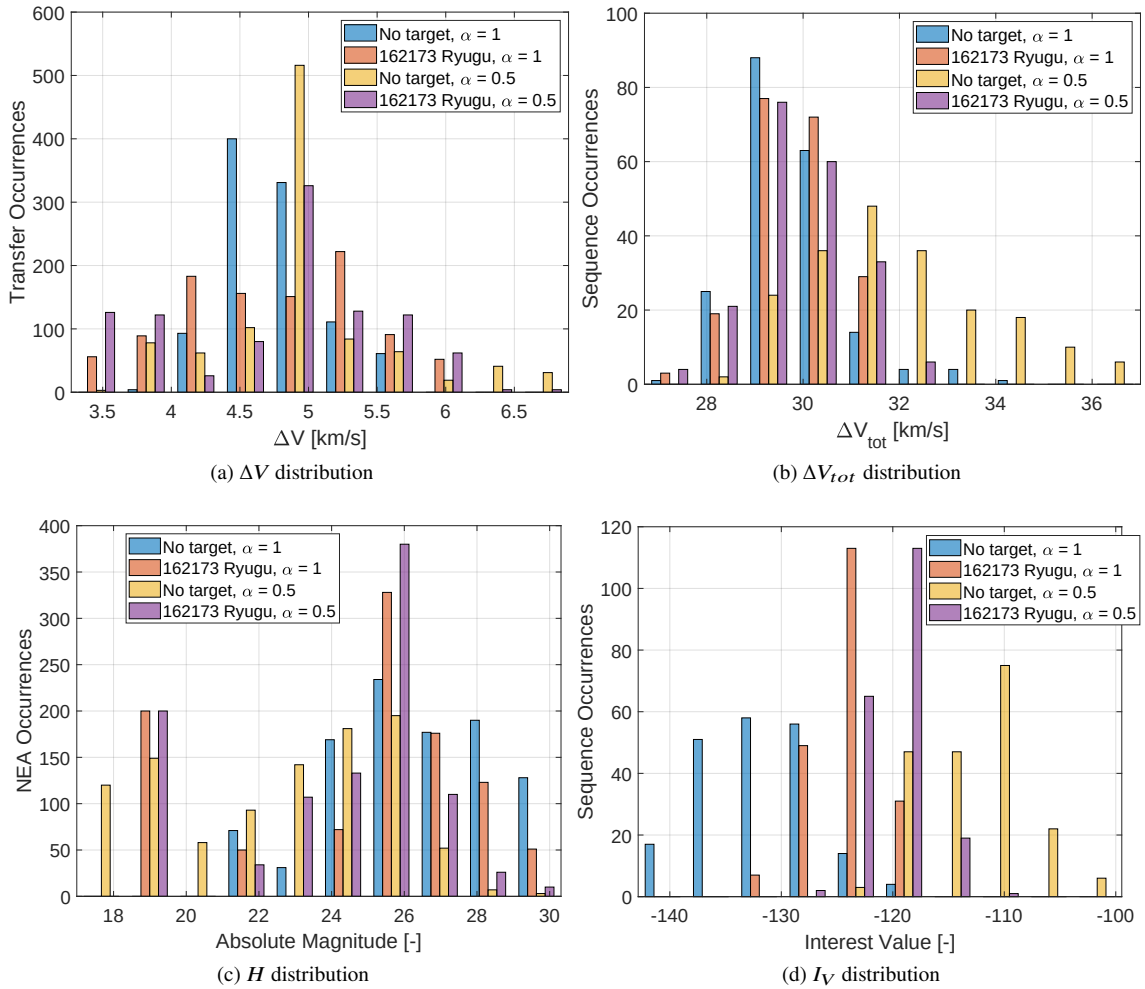

(a) ΔV distribution

(b) ΔV_{tot} distribution

(c) H distribution

(d) I_V distribution

Fig. 8 Distribution of the ΔV (a), ΔV_{tot} (b), absolute magnitude H (c) and interest value I_V (d) of the obtained sequences and NEAs visited.

IV. Multiple NEA Sample Return Missions

To verify the outcome of the sequence search algorithm, three sequences are selected and fully optimized for a solar electric propulsion system with maximum thrust $T_{max} = 0.3$ N, specific impulse $I_{sp} = 3000$ s, and initial mass $m_0 = 1500$ kg. The sequences are selected from the following simulations:

1) Sequence A, chosen as the sequence with lowest ΔV obtained from case (1) (sequence search with no target asteroid and $\alpha = 1$)
2) Sequence B, chosen as the sequence with lowest ΔV obtained from case (2) (sequence search with 162173 Ryugu as the target asteroid and $\alpha = 1$)
3) Sequence C, chosen as the sequence with greater I_V obtained from case (3) (sequence search with no the target asteroid and $\alpha = 0.5$)

The orbital characteristics of the asteroids visited during the Sequences A, B and C are detailed in Tables 2, 3 and 4,

Table 2 Characteristics of the NEAs visited in Sequence A.

Sequence A	2008 EA9	2010 AN61	2018 CQ3	2004 FM32	2015 VO142
a, AU	1.05	1.16	1.17	1.10	1.08
e, -	0.07	0.13	0.15	0.16	0.13
i, deg	0.44	3.61	4.00	3.76	0.28
H, -	27.7	27.0	25.2	27.1	28.9
Estimated size, m	8-19	11-24	27-60	11-24	4-10
PHA	No	No	No	No	No
NHATS	Yes	Yes	Yes	Yes	Yes
Orbit Class	Apollo	Apollo	Apollo	Apollo	Apollo

Table 3 Characteristics of the NEAs visited in Sequence B.

Sequence B	2016 TB18	1998 KG3	162173 Ryugu	2014 UY	2008 EA9
a, AU	1.08	1.16	1.19	1.17	1.05
e, -	0.08	0.12	0.19	0.17	0.07
i, deg	1.53	5.51	5.88	3.56	0.44
H, -	24.8	22.1	19.3	25.4	27.7
Estimated size, m	27-60	110-240	870-1000	21-48	8-19
PHA	No	No	Yes	No	No
NHATS	Yes	Yes	Yes	Yes	Yes
Orbit Class	Apollo	Amor	Apollo	Apollo	Apollo

Table 4 Characteristics of the NEAs visited in Sequence C.

Sequence C	1998 KG3	162173 Ryugu	2017 UY4	2000 LY27	2001 QC34
a, AU	1.16	1.19	1.19	1.31	1.13
e, -	0.12	0.19	0.16	0.21	0.19
i, deg	5.51	5.88	3.78	9.02	6.24
H, -	22.1	19.3	25.2	17.0	20.1
Estimated size, m	110-240	870-1000	27-60	1100-2400	270-600
PHA	No	Yes	No	Yes	Yes
NHATS	Yes	Yes	Yes	No	Yes
Orbit Class	Amor	Apollo	Apollo	Amor	Apollo

respectively. The sequences visit five asteroids, of which some are PHA and all are NHATS except for 2000 LY27, which is a PHA and presents the lowest absolute magnitude H. The estimated size of the asteroids is calculated using Eq. (10) and taking into account an albedo between 0.05 and 0.25.

The low-thrust OCP is solved to find the high-fidelity trajectories. The dynamics is described by the following set of ordinary differential equations:

Table 5 Mission parameters of the optimized NEA Sequence A. Comparison of optimal results with ANN estimations (in brackets).

Leg	Departure	Arrival	TOF, days	ΔV, km/s	Stay Time, days
Earth - 2008 EA9	2035-08-24	2037-04-20	605 (545)	5.96 (5.48)	83
2008 EA9 - 2010 AN61	2037-07-12	2038-11-29	505 (560)	4.80 (4.61)	20
2010 AN61 - 2018 CQ3	2038-12-19	2040-08-19	609 (550)	4.47 (4.43)	20
2018 CQ3 - 2004 FM32	2040-09-08	2042-06-08	638 (558)	4.75 (4.63)	100
2004 FM32 - 2015 VO142	2042-09-16	2043-10-05	384 (368)	3.10 (3.61)	54
2015 VO142 - Earth	2043-11-28	2045-03-31	489 (489)	4.01 (4.34)	–

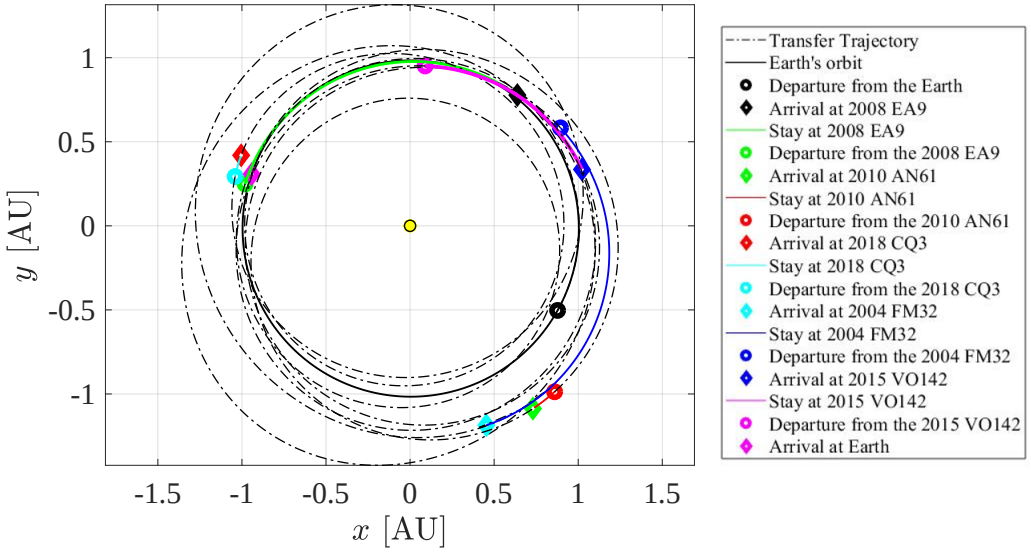

Fig. 9 Sequence A with no asteroid targeting and α = 1: heliocentric ecliptic-plane view.

$$\dot{\mathbf{x}}(t) = \mathbf{A}(\mathbf{x})\mathbf{a_T} + \mathbf{b}(\mathbf{x}) \tag{13}$$

where $\mathbf{x}$ is the state vector of the system, expressed in modified equinoctial elements and the spacecraft mass, $\mathbf{A}(\mathbf{x})$ and $\mathbf{b}(\mathbf{x})$ are, respectively, the matrix and the vector of the dynamics, as defined in Ref. [38]. The acceleration generated by the SEP system $\mathbf{a}_T$ can be described as follows:

$$\mathbf{a_T} = \frac{T_{max}}{m}\mathbf{N} \tag{14}$$

where T_{max} is the maximum thrust that can be generated and $\mathbf{N}$ is the normalized acceleration vector. The magnitude of

Table 6 Mission parameters of the optimized NEA Sequence B. Comparison of optimal results with ANN estimations (in brackets).

Leg	Departure	Arrival	TOF, days	ΔV, km/s	Stay Time, days
Earth - 2016 TB18	2035-09-13	2036-11-07	421 (444)	2.51 (2.97)	47
2016 TB18 - 1998 KG3	2036-12-24	2038-04-24	486 (456)	9.89 (5.57)	43
1998 KG3 - 162173 Ryugu	2038-06-06	2039-05-27	355 (355)	4.30 (3.97)	65
162173 Ryugu - 2014 UY	2039-07-31	2040-03-23	236 (302)	2.49 (2.70)	28
2014 UY - 2008 EA9	2040-04-20	2041-09-14	512 (532)	4.94 (4.59)	117
2008 EA9 - Earth	2042-01-09	2043-01-26	382 (362)	2.61 (2.73)	–

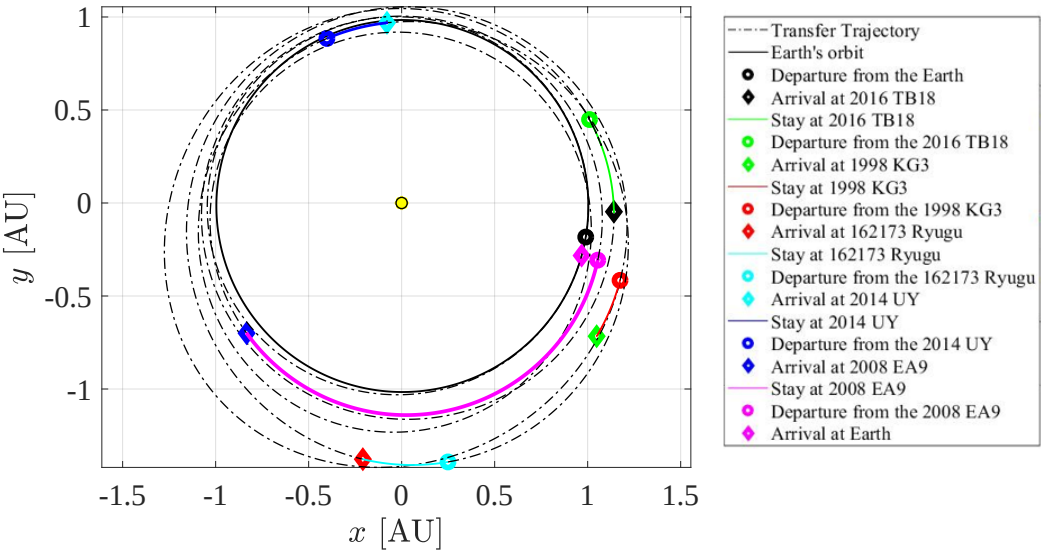

Fig. 10 Sequence B with target 162173 Ryugu and α = 1: heliocentric ecliptic-plane view.

N is bounded so that $0 < ||\mathbf{N}|| < 1$ to allow for thrust throttling and its radial, transverse and out-of-plane components are bounded within the interval $[-1, 1]$. The acceleration $\mathbf{a}_T$ is considered to be available at any time and regardless of the Sun distance.

The mass m of the spacecraft varies with time due to thrusting and can be described by the following mass differential equation:

$$\dot{m} = -\frac{T_{max}|\mathbf{N}|}{I_{sp} g_0} \tag{15}$$

The OCP is solved by using GPOPS, which uses a discrete non-linear programming (NLP) together with a variable-

Table 7 Mission parameters of the optimized NEA Sequence C. Comparison of optimal results with ANN estimations (in brackets).

Leg	Departure	Arrival	TOF, days	ΔV, km/s	Stay Time, days
Earth - 1998 KG3	2035-09-11	2037-06-09	637 (655)	6.51 (6.81)	86
1998 KG3 - 162173 Ryugu	2037-09-03	2039-01-01	485 (405)	5.31 (4.94)	47
162173 Ryugu - 2017 UY4	2039-02-17	2040-07-24	523 (543)	5.79 (5.90)	98
2017 UY4 - 2000 LY27	2040-10-30	2042-07-23	631 (651)	5.68 (5.17)	120
2000 LY27 - 2001 QC34	2042-11-20	2044-09-12	662 (582)	7.29 (6.49)	109
2001 QC34 - Earth	2044-12-30	2046-01-20	386 (386)	5.87 (5.53)	–

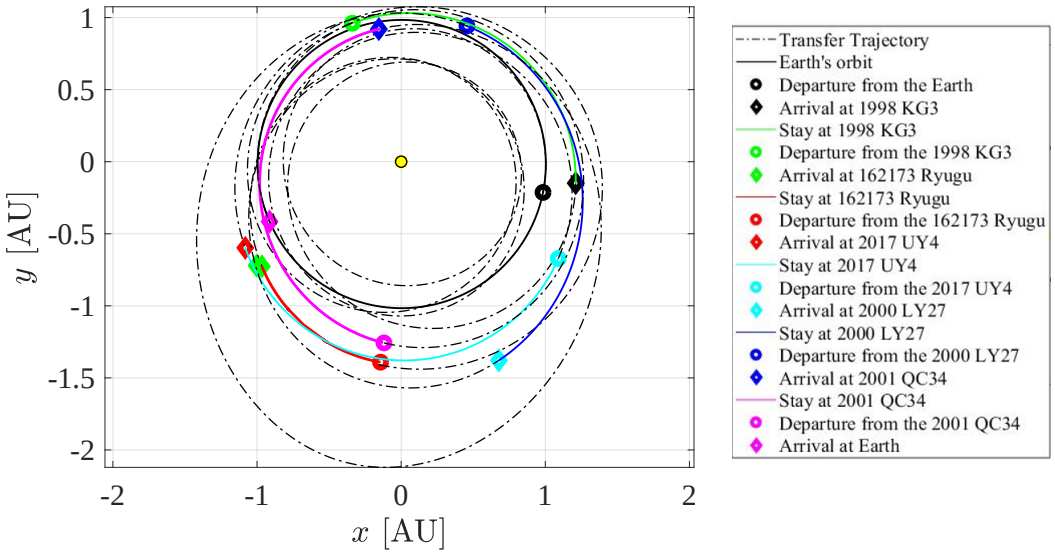

Fig. 11 Sequence C with no asteroid targeting and α = 0.5: heliocentric ecliptic-plane view.

order adaptive Radau collocation method [39] and the NLP solver IPOPT [40]. The objective of the optimization algorithm is to find the optimal control vector that minimizes the total mass expenditure while fulfilling the dynamics constraints of Eq.(14) at any time. The optimization is performed on the trajectory leg by leg sequentially, starting from an initial guess which is generated by solving a Lambert problem [41], where the TOF estimated by the ANN is used. The initial position of the spacecraft is set equal to the position of the departure body at the given departure date. In the first leg, Earth is the departure body and the departure date is the fixed launch date selected by the mission designer and used in the sequence search algorithm (a systematic search could be performed over a launch window); in the following legs, the departure body is the previously-visited asteroid and the departure date is the sum of the fixed launch date and the optimal transfer time of the previous legs. To allow enough time for close-up observations and/or sample collection

a minimum stay time of 20 days is enforced.

Tables 5, 6 and 7 describe the optimized mission characteristics of Sequence A, B and C, respectively. The departure and arrival dates (in YYYY-MM-DD format), the TOF, the ΔV and stay time are specified for each transfer. To compare the optimized values with those estimated by the ANN, the latter are expressed within brackets. The optimization procedure was able to find a solution for each of the transfers involved, showing that the trajectories are feasible and the spacecraft can return to Earth after visiting five asteroids within ten years from departure. The heliocentric ecliptic-plane view of the optimized trajectories for Sequence A, B and C are shown in Fig. 9, 10 and 11.

The sequence search algorithm generates $N_S = 200$ asteroid sequences in about 7.6 hours and 3.3 hours for the cases in which no asteroid or an asteroid is targeted during the search, respectively. The simulations have been performed on a machine with a Core i7 processor at 3.4 GHz. In previous works of the authors [25, 42], the required computational time when an ANN is used in the sequence search has been compared with the time required for other previously used methodologies [13], which typically required tens of days for a similar simulation to fully compute the multiple NEA sequences. When ANN is used, the algorithm results to be *two* orders of magnitude *faster*, when a couple of thousands objects are considered in the database.

To evaluate how well the network performs with respect to the optimization procedure, the deviations of the TOF and ΔV between the values estimated by the ANN and the optimal ones are calculated as the average percentage errors, i.e.:

$$\mathcal{E}_{TOF} = \frac{1}{N}\sum_{i=1}^{N}\left(\frac{|TOF_{i,opt} - TOF_{i,ANN}|}{TOF_{i,opt}}\right) \tag{16}$$

$$\mathcal{E}_{\Delta V} = \frac{1}{N}\sum_{i=1}^{N}\left(\frac{|\Delta V_{i,opt} - \Delta V_{i,ANN}|}{\Delta V_{i,opt}}\right) \tag{17}$$

with N being the number of legs in the trajectory.

Table 8 presents the percentage errors of the three sequences, together with a summary of the total ΔV and I_V for each of them. It can be noted again that, to fly NEA rendezvous missions with greater I_V, thus visiting asteroids of larger sizes, a larger ΔV is generally required which is however still achievable with the chosen propulsion system. The mean error of the Sequences A, B and C is 7.46% for the TOF estimation and 7.27% for the ΔV estimation. It can be concluded that the trained network is able to estimate with a reasonably accuracy the cost and duration of transfers from the Earth, between NEAs and back to the Earth, while greatly reducing the computational time.

V. Conclusions

An artificial neural network is designed and used to *quickly* estimate the cost and duration of low-thrust, rendezvous transfers between near-Earth asteroids. The network, whose architecture is optimized for this application, is integrated with the sequence search algorithm which, based on a tree-search method, can identify the most convenient sequences

Table 8 Total ΔV and I_V of the selected sequences with the average percentage error between ANN and the optimized results.

Sequence	ΔV_{tot}	I_V	$\mathcal{E}_{TOF}$	$\mathcal{E}_{\Delta V}$
A (Table 5)	28.11	-135.9	7.87%	6.69%
B (Table 6)	27.35	-119.3	8.12%	8.59%
C (Table 7)	35.75	-103.7	6.40%	6.54%
Mean Error	–	–	**7.46%**	**7.27%**

from the point of view of the mass expenditure and/or the interest value of the asteroids visited. In this work, an asteroid is considered more *interesting* if it is larger, i.e., lower absolute magnitude and greater interest value, I_V.

The sequence search algorithm is designed so that, while visiting a defined number of asteroids in a set amount of time, it directs the spacecraft towards asteroids that are closer (in the orbital parameter space) to a target asteroid or, if in the final leg, to Earth and eventually transfer to Earth itself. At each leg, the search retains the best 200 sequences in terms of the appealing factor, i.e., the weighted sum of the interest value and ΔV. Changing the value of the weight coefficient affects the importance given to I_V and ΔV in the sequence selection process.

The analysis of the distribution of the total ΔV and I_V of the obtained sequences reveals that, when the selection of the sequences during the search is made on the basis of both the I_V and ΔV, more interesting objects can be visited, increasing the overall appeal of the sequences at the cost of a larger ΔV. Three sequences were analyzed and fully optimized, to obtain the flight trajectory and control history. It is shown that employing machine learning techniques within the sequence search algorithm greatly reduces the computational time, while still ensuring a high accuracy with an average percentage error of about 7% with respect to the optimal values.

VI. Acknowledgments

Giulia Viavattene gratefully acknowledges the support received for this research from the James Watt School of Engineering at the University of Glasgow for funding the research under the James Watt sponsorship program.

References

[1] Chaikin, A., *A Man On the Moon: The Voyages of the Apollo Astronauts*, 3rd ed., New York: Penguin Books, 2007.

[2] Lauretta, D., "OSIRIS-REx Asteroid Sample-Return Mission," *Handbook of Cosmic Hazards and Planetary Defense*, 2015, pp. 543–567. https://doi.org/10.1007/978-3-319-03952-744.

[3] Lissauer, J. J., and de Parter, I., *Fundamental Plantary Science*, Cambridge University Press, 2013.

[4] Yoshikawa, M., Kawaguchi, J., and Fujiwara. A., "Hayabusa Sample Return Mission," *Asteroids IV*, 2015, pp. 397–418. https://doi.org/10.2458/azu-uapress-9780816532131-ch021.

[5] Tsuda, Y., Yoshikawa, M., Abe, M., Minamino, H. and Nakazawa, S., "System design of the Hayabusa 2: Asteroid sample return mission to 1999 JU3," *Acta Astronautica*, Vol. 91, 2013, pp. 356–362. https://doi.org/10.1016/j.actaastro.2013.06.028.

[6] McInnes, C. R., *Solar Sailing - Technology, Dynamics and Mission Applications*, 1999. https://doi.org/10.1007/978-1-4471-3992-8.

[7] Mereta, A., and Izzo, D., "Target selection for a small low-thrust mission to near-Earth asteroids," *Astrodynamics*, Vol. 2, No. 3, 2018, pp. 249–263.

[8] Izzo, D., Simoes, L. F., Yam, C. H., Biscani, F., Di Lorenzo, D., Bernardetta, A., and Cassioli, A., "GTOC5 : Results from the European Space Agency and University of Florence," *Acta Futura*, Vol. 8, No. November, 2014, pp. 45–56. https://doi.org/10.2420/AF08.2014.45.

[9] Wertz, J. R., *Orbit & Constellation Design & Management*, Springer, New York, 2009.

[10] Jahn, R. G., *Physics of Electric Propulsion*, McGraw-Hill Book Company, New York, 2006.

[11] Yang, H., Tang, G., and F. Jiang, "Optimization of observing sequence based on nominal trajectories of symmetric observing configuration," *Astrodynamics*, Vol. 2, No. 1, 2018, pp. 25–37. https://doi.org/10.1007/S42064-017-0009-2.

[12] Li, H., Chen, S., Izzo, D., and Baoyin, H., "Deep Networks as Approximators of Optimal Transfers Solutions in Multitarget Missions," *Acta Astronautica*, 2019. https://doi.org/10.1016/j.actaastro.2019.09.023.

[13] Peloni, A., Ceriotti, M., and Dachwald, B., "Solar-Sail Trajectory Design for a Multiple Near-Earth-Asteroid Rendezvous Mission," *Journal of Guidance, Control, and Dynamics*, Vol. 39, No. 12, 2016, pp. 2712–2724. https://doi.org/10.2514/1.G000470.

[14] Tang, G., Jiang, F., and Li, J., "Trajectory Optimization for Low-Thrust Multiple Asteroids Rendezvous Mission," *AIAA/AAS Astrodynamics Specialist Conference*, 2015. https://doi.org/10.1515/jnum-2014-0003.

[15] Di Carlo, M., Martin, J. M. R., Gomez, N., and Vasile, M., "Optimised Low-Thrust Mission to the Atira Asteroids," *Advances in Space Research*, Vol. 59, 2017, pp. 1724–1739. https://doi.org/10.1016/j.asr.2017.01.009.

[16] Izzo, D., Martens, M., and Pan, B., "A Survey on Artificial Intelligence Trends in Spacecraft Guidance Dynamics and Control," *Springer, Astrodynamics*, , No. 3, 2019, pp. 287–299. https://doi.org/10.1007/s42064-018-0053-6.

[17] Dachwald, B., "Optimization of Interplanetary Solar Sailcraft Trajectories," *Journal of Guidance, Control, and Dynamics*, Vol. 27, No. 1, 2004. https://doi.org/10.2514/1.9286.

[18] Hennes, D., Izzo, D., and Landau, D., "Fast Approximators for Optimal Low-Thrust Hops Between Main Belt Asteroids," *IEEE Symposium Series on Computational Intelligence (SSCI)*, 2016. https://doi.org/10.1109/SSCI.2016.7850107.

[19] Mereta, A., Izzo, D., and Wittig, A., "Machine Learning of Optimal Low-Thrust Transfers Between Near-Earth Objects," *Hybrid Artificial Intelligent Systems*, 2017, pp. 543–553. https://doi.org/10.1007/978-3-319-59650-146.

[20] Sánchez-Sánchez, C., and Izzo, D., "Real-time optimal control via Deep Neural Networks: study on landing problems," *Journal of Guidance, Control, and Dynamics*, Vol. 41, No. 3, 2018, pp. 1122–1135. https://doi.org/10.1023/B:CJOP.0000010527.13037.22, URL http://arxiv.org/abs/1610.08668.

[21] Peng, H., and Bai, X., "Artificial Neural Network–Based Machine Learning Approach to Improve Orbit Prediction Accuracy," *AIAA Journal of Spacecraft and Rockets*, Vol. 55, No. 5, 2018, pp. 1–13. https://doi.org/10.2514/1.A34171.

[22] Song, Y., and Gong, S., "Solar-Sail Trajectory Design of Multiple Near Earth Asteroids Exploration Based on Deep Neural Network," *Aerospace Science and Technology*, Vol. 91, 2019, pp. 28–40. https://doi.org/10.1016/j.ast.2019.04.056.

[23] Viavattene, G., and Ceriotti, M., "Artificial Neural Network for Preliminary Multiple NEA Rendezvous Mission Using Low Thrust," *70th International Astronautical Congress (IAC), Washington DC, USA*, 2019.

[24] Viavattene, G., and Ceriotti, M., "Artificial neural network design for tours of multiple asteroids," *Springer, Lectures Notes in Computer Science*, 2020. https://doi.org/10.1007/978-3-030-61705-9_63.

[25] Viavattene, G., and Ceriotti, M., "Artificial Neural Networks for Multiple NEA Rendezvous Missions with Continuous Thrust," *AIAA Journal of Spacecraft and Rockets*, 2021. https://doi.org/10.2514/1.A34799.

[26] Grigoriev, I.S. and Zapletin, M.P., "Choosing promising sequences of asteroids," *Automation and Remote Control*, Vol. 8, No. 74, 2014, pp. 1284–1296.

[27] Petropoulos, A.E. and Bonfiglio, E.P. and Grebow, D.J. and Lam, T. and Parker, J.S. and Arrieta, J. and Landau, D.F. and Anderson, R.L. and Gustafson, E.D. and Whiffen, G.J. and Finlayson, P.A. and Sims, J.A., "GTOC5: Results from the Jet Propulsion Laboratory," *Acta Futura*, Vol. 8, No. November, 2014, pp. 21–27.

[28] Izzo, D., Hennes, D., Simões, L. F., and Märtens, M., "Designing complex interplanetary trajectories for the Global Trajectory Optimization competitions," *Springer Optimization and Its Applications*, Vol. 114, 2016, pp. 151–176. https://doi.org/10.1007/978-3-319-41508-6_6.

[29] Rutkowski, L., Korytkowski, M., Scherer, R., Tadeusiewicz, R., Zadeh, L. A., and Zurada, J. M., *Artificial Intelligence and Soft Computing*, Springer, Zakopane, Poland, 2013. https://doi.org/10.1007/978-3-642-38658-9.

[30] Goodfellow, I., Bengio, Y., and Courville, A., *Deep Learning*, The MIT Press, Cambridge, Massachusetts, 2016.

[31] Rojas, R., *Neural Networks: A Systemic Introduction*, Springer, New York, 1996. https://doi.org/10.1016/0893-6080(94)90051-5.

[32] Wiesel, W., *Spaceflight Dynamics: Third Edition*, CreateSpace, Cambridge, Massachusetts, 2017.

[33] De Pascale, P., and Vasile, M., "Preliminary Design of Low-Thrust Multiple Gravity-Assist Trajectories," *AIAA Journal of Spacecraft and Rockets*, Vol. 43, No. 5, 2006, pp. 1065–1076. https://doi.org/10.2514/1.19646.

[34] Vilas, F., "Spectral characteristics of Hayabusa 2 near-Earth asteroid targets 162173 1999 JU3 AND 2001 QC34," *The Astronomical Journal*, Vol. 135, 2008, pp. 1101–1105. https://doi.org/10.1088/0004-6256/135/4/1101.

[35] Tholen, D. J., and Barucci, M. A., "Asteroid taxonomy," *Asteroids II, Proceedings of the Conference*, , No. March, 1989, pp. 298–315.

[36] Harris, A. W., and Harris, A. W., "On the Revision of Radiometric Albedos and Diameters of Asteroids," *Icarus*, Vol. 126, No. 2, 1997, pp. 450–454. https://doi.org/10.1006/icar.1996.5664.

[37] Chesley, S. R., Chodas, P. W., Milani, A., Valsecchi, G. B., and Yeomans, D. K., "Quantifying the Risk Posed by Potential Earth Impacts," *Icarus*, Vol. 159, No. 2, 2002, pp. 423–432. https://doi.org/10.1006/icar.2002.6910.

[38] Betts, J. T., *Practical Methods for Optimal Control and Estimation Using Nonlinear Programming*, 2nd ed., SIAM Press, Philadelphia, 2010.

[39] Patterson, M. A., and Rao, A. V., "GPOPS-II: A MATLAB Software for Solving Multiple-Phase Optimal Control Problems usign hp-Adaptive Gaussian Quadrature Collocation Methods and Sparse Nonlinear Programming," *ACM Transactions on Mathematical Software*, Vol. 41, No. 1, 2014. https://doi.org/10.1145/2558904.

[40] Wachter, A., and Biegler, L. T., "On the Implementation of an Interior-Point Filter Line-search Algorithm for Large-scale Non-linear Programming," *Mathematical Programming*, Vol. 106, No. 1, 2006, pp. 25–57. https://doi.org/10.1007/s10107-004-0559-y.

[41] Curtis, H., *Orbital Mechanics for Engineering Students*, Elsevier, 2005.

[42] Viavattene, G., Devereux, E., Snelling, D., Payne, N., Wokes, S., and Ceriotti, M., "Design of Multiple Space Debris Removal Missions using Machine Learning," *Acta Astronautica*, Vol. 193, 2022, pp. 277–289. https://doi.org/10.1016/j.actaastro.2021.12.051.